

## PHASE AND SURFACE MODIFICATION BY ELECTROCHEMICAL POST DEPOSITION TREATMENTS IN ULTRASONIC-ASSISTED CuInSe<sub>2</sub>/Cu ELECTRODEPOSITED FILMS

L.E. ARVIZU-RODRÍGUEZ<sup>a</sup>, A. PALACIOS-PADRÓS<sup>b</sup>, F. CHALÉ-LARA<sup>a</sup>,  
J. L. FERNÁNDEZ-MUÑOZ<sup>c</sup>, I. DÍEZ-PÉREZ<sup>b</sup>, F. SANZ<sup>d,e,b</sup>,  
F. J. ESPINOSA-FALLER<sup>e</sup>, J. SANDOVAL<sup>f</sup>, F. CABALLERO-BRIONES<sup>a\*</sup>

<sup>a</sup>*Instituto Politécnico Nacional, Laboratorio de Materiales Fotovoltaicos, CICATA Altamira. Km 14.5 Carretera Tampico-Puerto Industrial Altamira. 89600 Altamira, México*

<sup>b</sup>*Departament de Química Física, Universitat de Barcelona, Martí i Franquès 1, 08028, Barcelona, Spain*

<sup>c</sup>*Instituto Politécnico Nacional, CICATA Legaria. Calzada Legaria 396 Col. Irrigación, 11500 México DF México.*

<sup>d</sup>*Institute for Bioengineering of Catalonia (IBEC), Edifici Hèlix, Baldori i Reixac 15-21, 08028 Barcelona, Spain*

<sup>e</sup>*CIBER-BBN, Campus Río Ebro Edificio I+D, Bloque 5, 1a planta, C/Poeta Mariano Esquillor s/n, 50018 Spain*

<sup>e</sup>*Unidad Experimental Marista, Laboratorio de Materiales, Sensores y Películas Delgadas, Universidad Marista de Mérida, Periférico Norte Tablaje 13941, Mérida, 97300 México.*

<sup>f</sup>*CINVESTAV-IPN Unidad Querétaro, Libramiento Norponiente, Fracc. Real de Juriquilla, Juriquilla, México*

CuInSe<sub>2</sub> films were prepared onto Cu-cladded substrates by ultrasonic-assisted electrodeposition using different bath compositions and a fixed deposition potential of E=-1500 mV vs Ag/AgCl. *In situ* electrochemical treatments named selenization and electrocrystallization, in a Se<sup>4+</sup> electrolyte were applied to modify the morphology, film structure and the phase composition. Films were characterized by scanning electron microscopy, X-ray diffraction, Raman spectroscopy and photocurrent response. A Cu<sub>2-x</sub>Se layer develops as the electrode is introduced into the electrolyte. The presence of Cu-In, In-Se, Cu-Se, cubic, hexagonal and tetragonal CuInSe<sub>2</sub> phases as well as elemental In and Se was observed. After selenization, partial phase dissolution and Se deposition is observed and after the electrocrystallization treatment the secondary phases such as Cu-Se, Cu-In, In and Se reduce substantially and the grain sizes increase, as well as the photocurrent response. Phase diagrams are constructed for each set of films and reaction mechanisms are proposed to explain the phase evolution.

(Received June 30, 2015; Accepted October 31, 2015)

**Keywords.** CuInSe<sub>2</sub>, electrodeposition, in situ electrochemical treatments, Surface modification, phase composition

### 1. Introduction

Electrodeposition has been pointed out as a promising alternative for CuInSe<sub>2</sub> (CIS) absorbers for thin film solar cells, owing to the lower investment and materials costs. Overall, solar cell efficiencies up to 10.6% can be achieved for CIS [1]. In this line, reported approaches include

---

\*Corresponding author: fcaballero@ipn.mx

the deposition of stacked Cu and In layers [2,3], one step electrodeposition of CIS [4] or even deposition with potential pulses [5]. Ultrasonic assistance has been used during electrodeposition of semiconducting films [6], metal alloys [3] and nanoparticles [7], in order to produce cavitation, microstreaming and degassing, all of which can clean electrode, reduce concentration polarization as the diffusion layer thickness reduces, and the overall cathodic current efficiency improves [3,7]. Moreover, it has been reported that simple baths without additives or surfactants, can be used to prepare homogenous thin films due to the effects of ultrasonic irradiation [6]. Hydrogen can be used as a fast gentle and controllable surface cleaning. Hydrogen is able to remove the binary phases CuS and CuSe from the surface [8], for that reason growing at very cathode potential is proposed to allow evolution of hydrogen. All the CIS electrodeposition processes, though, are usually followed by an annealing process in Se atmosphere and a KCN etching to remove undesired Se and Cu-Se remnants [2,4] with the inconvenience of using toxic materials and off-the-line operations. Pulsed electrodeposition has shown to reduce the presence of such phases [5], but pulsed sources are not always easily available and limited supply of reactants to the electrodes can occur at long term deposition.

On the other hand, CuInSe<sub>2</sub> solar cells are usually prepared onto Mo/glass substrates, but in order to reduce costs, CuInS<sub>2</sub> solar cells have recently been prepared onto Cu tape [8] and efficiencies as high as 9% have been reached, indicating that large scale production of CIS/Cu based cells is feasible.

In this work, ultrasonic assisted electrodeposition of CIS films is done onto Cu substrates varying the Cu:Se:In proportion in a simple solution free of complexing agents. The ultrasonic assistance is used to enhance the compactness of the films, remove H<sub>2</sub> produced at the deposition potential and keep a constant supply of reactants at the electrode surface. Post-deposition electrochemical treatments in a Se<sup>4+</sup> electrolyte were performed in analogy to the processes reported for Cu<sub>2-x</sub>Te/Cu films [9] to modify the phase composition of the films [10], so with accurate optimization, the presence of unwanted Cu-Se phases could be considerably reduced.

## 2. Experimental details

Films were prepared onto 0.8 mm thick, single-sided PC boards (Pulsar Pro, FL) with 75 μm thick cladded Cu. Prior to electrodeposition, Cu was chemically polished during 20s in a 0.5% V/V H<sub>2</sub>SO<sub>4</sub> + 25% H<sub>2</sub>O<sub>2</sub> solution under sonication and immediately dipped into a 5% V/V H<sub>2</sub>SO<sub>4</sub> solution to remove the oxide. Finally the substrates were rinsed with DI water and N<sub>2</sub> blown. Deposition was done using a home-made potentiostat [12] in the three electrode configuration: 10 x 25 mm<sup>2</sup> pieces of the Cu-cladded board were used as working electrode, a 25 x 25 mm<sup>2</sup> Pt gauze (Sigma Aldrich) acted as counter electrode and as reference a miniature Ag/AgCl electrode (Biologic, JP) filled with 3M KCl (E vs SHE=222 mV) was used. The potentials from herein will be quoted against this electrode. During the deposition, the cell was kept in fixed position into an ultrasonic cleaner (Baku 3550, China) operating at a frequency of 25 kHz with 50 W power.

Aqueous solutions of CuSO<sub>4</sub>, In<sub>2</sub>(SO<sub>4</sub>)<sub>3</sub>·3H<sub>2</sub>O and SeO<sub>2</sub> prepared from high purity reactants (99.9%, Sigma Aldrich) and desionized water, were used as precursors and the Cu<sup>2+</sup>:Se<sup>4+</sup>:In<sup>3+</sup> molar relation in the bath was set to 1:1:2, 1:1:4 and 1:1:5. In all cases the Cu<sup>2+</sup> concentration was 3 mM and no supporting electrolyte was used. Films were prepared by introducing the substrates into the electrolyte 2 min before applying potential; then the potential was swept from OCP to -1500 mV at 5 mVs<sup>-1</sup> and afterwards the potential was maintained during 15 min before take out the substrates, rinse and N<sub>2</sub>-blow the films.

H<sub>2</sub> evolution was observed during the deposition, but the films remain firmly attached under rinsing and blowing. To proceed with the post-deposition treatments, the electrolyte solution used for the deposition was removed from the cell and exchanged by a 3 mM SeO<sub>2</sub> solution. Here, two different strategies were followed: i) the so-called selenization process that consists in sweeping the potential from -200 mV to -800 mV at 5 mVs<sup>-1</sup> plus a 5 min hold or ii) the selenization process followed by a so-called electrocrystallization step performed by sweeping back the potential up to -200 mV at 5mVs<sup>-1</sup>, and keeping the potential 5 min. After these post-deposition steps, the samples were rinsed with deionized water and dry under N<sub>2</sub> stream. Table 1 resumes the prepared films.

Table 1. Summary of the experimental conditions for the  $\text{CuInSe}_2$  films

Cu:Se:In	As-grown	Selenized	Electrocrystallized
1:1:2	CIS1-2	CIS2-2	CIS3-2
1:1:4	CIS1-4	CIS2-4	CIS3-4
1:1:5	CIS1-5	CIS2-5	CIS3-5

Morphology was characterized in JEOL JSM 7100 FESEM at 15 kV. X-ray diffractograms were acquired in a Bruker D8 in the Bragg-Brentano geometry using  $\text{CuK}\alpha$  radiation. Raman spectroscopy was done in a LabRam Dilor using the 532 nm line of an Ar laser focused through a 50X objective providing  $\sim 2 \text{ mW/cm}^2$  power density.

Photocurrent response was evaluated in a 0.1 M  $\text{NaNO}_3$  electrolyte solution by sweeping the potential from OCP to -1300 mV at  $5 \text{ mVs}^{-1}$  under dark and light conditions in the continuous wave mode. Illumination was provided by a 200 W white source.

### 3. Results and discussion

Fig. 1 presents the cyclic voltamogram of the Cu substrate acquired in the Se electrolyte from OCP to -2000 mV. Cu and In voltammograms (not shown) feature essentially the expected behavior, *i.e.* a peak related to the metal deposition at the cathodic excursion followed by its corresponding dissolution when anodically sweeping back the potential.

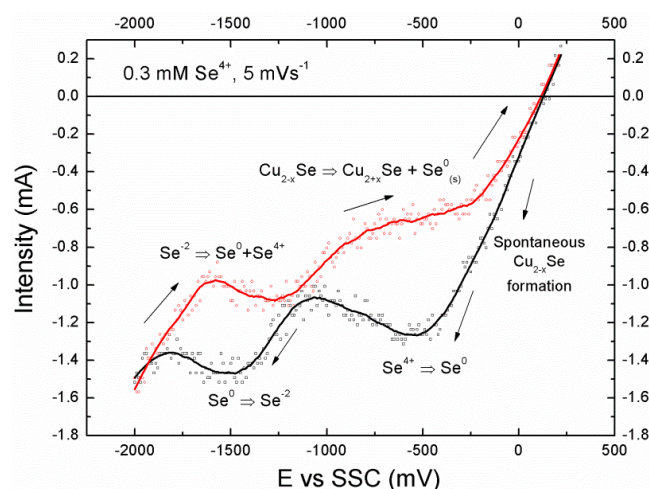


Fig. 1. Cyclic voltammogram of the Cu substrate into the  $\text{Se}^{4+}$  electrolyte

However, the voltammogram in  $\text{Se}^{4+}$  is remarkably different to that reported in [5]. As soon as the electrode is introduced in the Se electrolyte, a dark reddish film of  $\text{Cu}_{2-x}\text{Se}$  is formed, similarly to the behavior reported when Cu is immersed in a Te solution [9]. The voltammogram features two reduction waves at -500 mV and -1500 mV attributed to  $\text{Se}^{4+} \rightarrow \text{Se}^0$  and  $\text{Se}^0 \rightarrow \text{Se}^{2-}$  respectively. In the anodic excursion a wave corresponding to  $\text{Se}^{2-}$  disproportionation reaction to  $\text{Se}^0$  and  $\text{Se}^{4+}$  is observed [2].

The wave at around -1000 mV would correspond to oxidation of  $\text{Cu}_{2-x}\text{Se}$  to a substoichiometric  $\text{Cu}_{2+x}\text{Se}$  [2]. The negative current maintained during the anodic excursion indicates continuous Se deposition.

Fig. 2 presents the FESEM images of the prepared CIS films. From left to right images correspond to samples with an increasing In ratio in the bath and from top to bottom to the as-grown, selenized and electrocrystallized films, respectively.

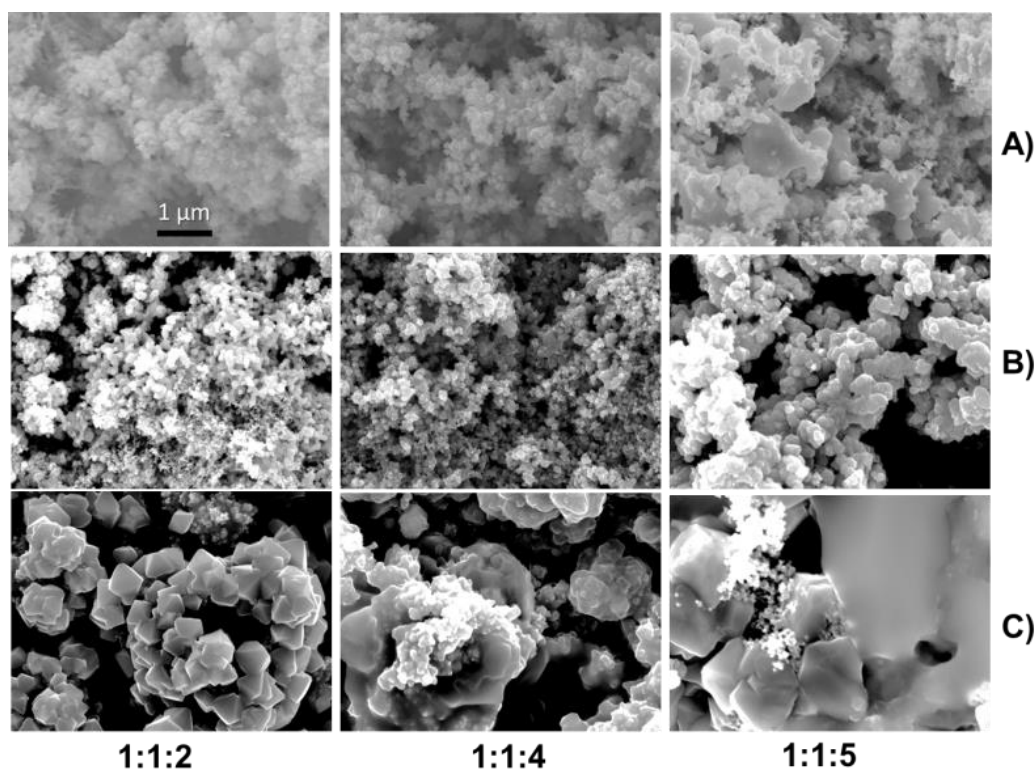


Fig. 2 FESEM micrographs of the  $\text{CuInSe}_2$  films. A) As-grown, B) Selenized and C) Electrocrystallized. Images in columns correspond to the Cu:Se:In proportions

Porous films composed of small grains that tend to increase in size when In content in the bath is raised were obtained. The porous nature is attributed to the  $\text{H}_2$  evolution during the growth process. After selenization, the porous morphology changes to small crystallites due to Se deposition. If a further electrocrystallization treatment is performed, then octahedral grains will be observed. In these conditions, grain coalescence and presence of flat plaques seem to increase with the In ratio in solution.

To see in more detail the variation of the morphology treatments, in Fig 3 the images obtained by atomic force microscopy are presented.

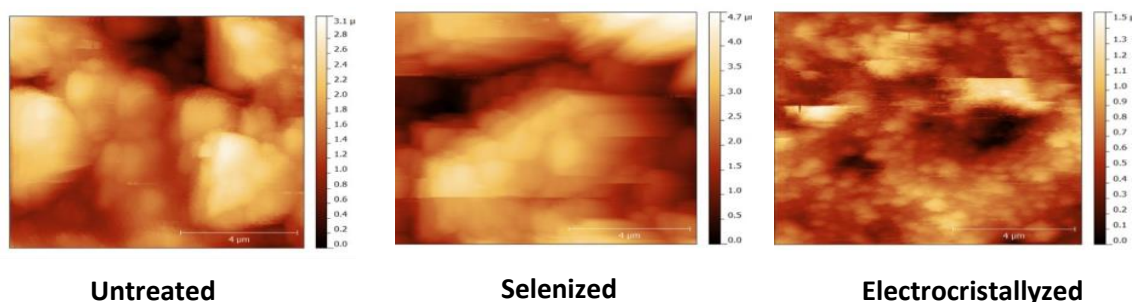


Fig. 3: AFM images of  $10 \times 10 \mu\text{m}^2$ .

It can be seen that treatment selenization causes coalescence of the grains but also the surface with more holes can be seen, consistent with corrosion observed by scanning electron microscopy. After electrocrystallization a surface composed of smaller grains is observed confirming that a renucleation of the materials dissolved during selenization occurs.

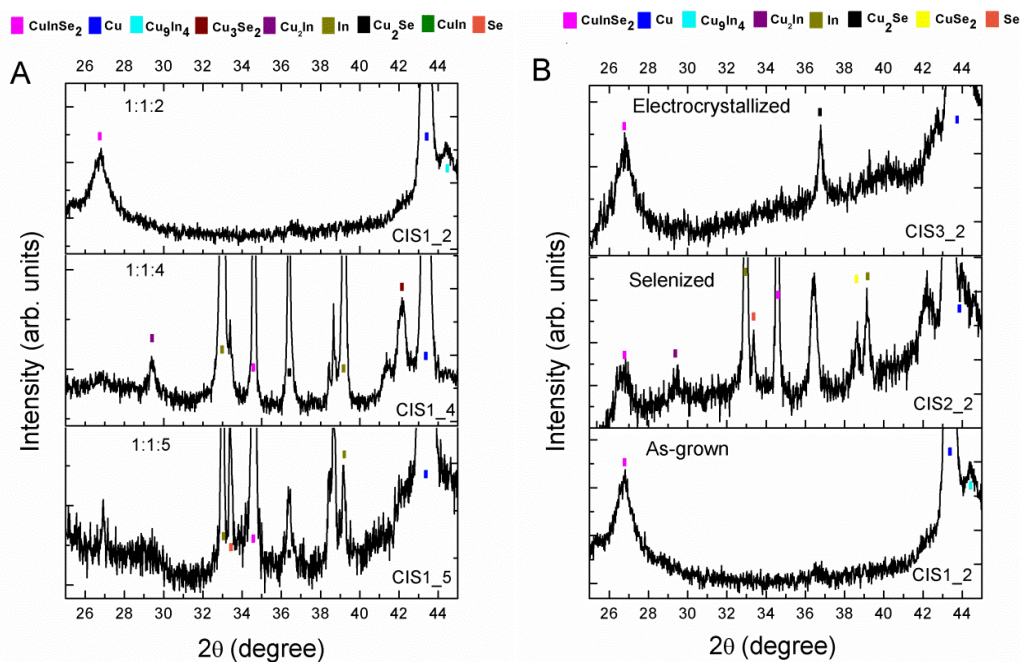


Fig. 4. X-ray diffractograms of A) As grown CIS films with increasing In contents in the bath; B) CIS films electrodeposited in the 1:1:2 bath

In the diffractogram of the film CIS1\_2 (Figure 4A) the peak corresponding to the tetragonal (112)  $\text{CuInSe}_2$  plane [12] can be observed. As the In proportion increases peaks corresponding to  $\text{Cu}_2\text{Se}$ ,  $\text{Cu}_2\text{In}$ ,  $\text{Cu}_9\text{In}_4$ ,  $\text{Cu}_3\text{Se}_2$ ,  $\text{CuSe}$ ,  $\text{Se}$  and  $\text{In}$  appear.

With the selenization treatment (Fig. 4B),  $\text{Cu}_2\text{Se}$  and  $\text{CuSe}_2$  peaks as well as  $\text{Se}$  and  $\text{In}$  peaks became evident. Upon electrocrystallization, all the secondary phases except  $\text{Cu}_2\text{Se}$  and  $\text{CuInSe}_2$  peaks disappear.

Raman spectra of all the films present bands associated with  $\text{InSe}$  compounds [2],  $\text{CuInSe}_2$  [13] and  $\text{Cu-Se}$  [10] at  $128\text{ cm}^{-1}$ ,  $178\text{ cm}^{-1}$  and  $261\text{ cm}^{-1}$ , respectively.

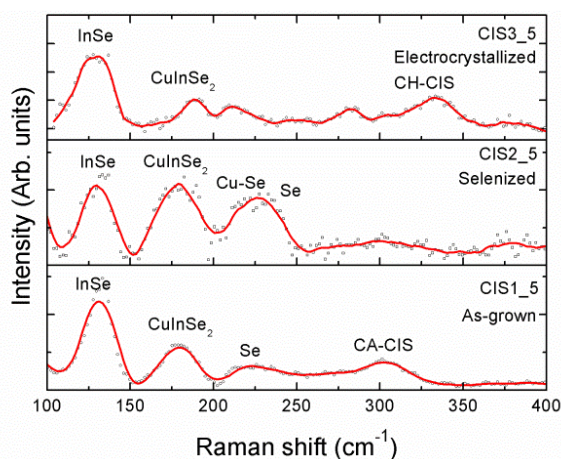


Fig. 5. Raman spectra of the CIS films prepared in the 1:1:5 bath, as-grown, selenized, electrocrystallized.

Wide bands associated to the  $\text{Cu}_3\text{Au}$  (CA) and cubic (CH) phases of  $\text{CuInSe}_2$  at around  $288\text{--}303\text{ cm}^{-1}$  and  $350\text{ cm}^{-1}$  are also evident [13]. Intense  $\text{InSe}$  bands can be the result of a quasi-resonance condition between  $\text{InSe}$  phases with optical band gap or  $2.3\text{ eV}$  ( $539\text{ nm}$ ) [5] and the  $532\text{ nm}$  laser, despite of the absence of defined  $\text{InSe}$  diffraction peaks. In the Raman spectra of the films CIS1\_5,

CIS2\_5 y CIS3\_5 (Figure 5), bands associated with In-Se at  $128\text{ cm}^{-1}$  reduce upon selenization and increase after electrocrystallization. Selenium band increases with the selenization treatment and after decreases after electrocrystallization. The relative intensity of the  $A_1$   $\text{CuInSe}_2$  band seems to decrease after electrocrystallization while the CH-CIS band increases.

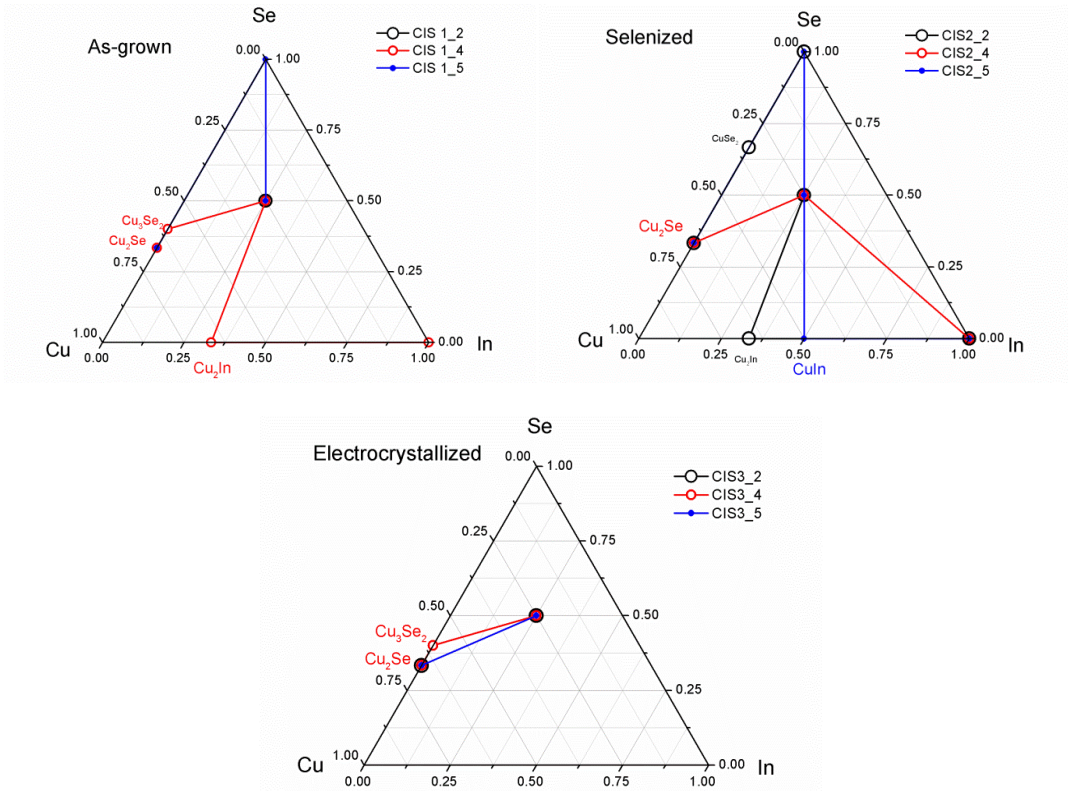


Fig. 6. Phase diagrams derived from XRD

Combining the qualitative results from the XRD and the Raman spectra, phase diagrams were constructed [14] as shown in Fig. 6(A-C). Table 2 presents the corresponding reaction mechanisms.

$\text{Cu}_2\text{Se}$  coming from the spontaneous reaction between Se and Cu and CIS is present in all the samples. It was observed that to ensure CIS adhesion, the formation of the  $\text{Cu}_2\text{Se}$  film onto the Cu substrate is necessary. An ohmic  $\text{Cu}_2\text{Se}$  interface between CIS and Cu is expected [9].

During the potential sweep from OCP to  $-1500\text{ mV}$  there is a competing formation of Cu-Se, In-Se and Cu-In phases as well as  $\text{CuInSe}_2$ . The In increase in the bath leads to the observed In and Cu-In deposits. Selenization seems to have the general effect of partially dissolving the phases formed during potential sweep including CIS and to deposit a Se excess that reacts with In and CuIn deposits to form Cu-Se and In-Se.

Table 2. Proposed reactions for the each electrochemical treatment

Electrodeposition	Selenization	Electrocrystallization
Stage 1: $\text{Se}_{\text{UPD}}$ , Cu-Se $2\text{Se}^{4+} + 2\text{Cu}^0 \leftrightarrow \text{Cu}_2\text{Se} + \text{Se}^0$ $\text{Se}^{4+} + \text{Cu}^{2+} + 6\text{e}^- \leftrightarrow \text{CuSe}$ $\text{Se}^0 + \text{Cu}^{2+} + 2\text{e}^- \leftrightarrow \text{CuSe}$ $\text{Se}^{4+} + 2\text{Cu}^{2+} + 8\text{e}^- \leftrightarrow \text{Cu}_2\text{Se}$ $\text{Se}^0 + 2\text{Cu}^{2+} + 4\text{e}^- \leftrightarrow \text{Cu}_2\text{Se}$ $2\text{CuSe} + \text{Se}^0 \rightarrow \text{Cu}_2\text{Se}_3$	Stage 1: $\text{Se}^{2-}$ formation $\text{Se}^0 \leftrightarrow \text{Se}^{2-} + 2\text{e}^-$	Stage 1. $\text{Se}^{2-}$ disproportionation $\text{Se}^0 + 2\text{e}^- \leftrightarrow \text{Se}^{2-}$ $\text{Se}^{2-} + \text{Se}^{4+} \leftrightarrow \text{Se}^0$
Stage 2: $\text{Se}^{2-}$ formation $2\text{CuSe} + 2\text{e}^- \leftrightarrow \text{Cu}_2\text{Se} + \text{Se}^{2-}$ $\text{Se}^0 \leftrightarrow \text{Se}^{2-} + 2\text{e}^-$	Stage 2. CuSe, $\text{Cu}_2\text{Se}$ , Se $\text{Se}^0 + \text{Cu}^{2+} + 2\text{e}^- \leftrightarrow \text{CuSe}$ $\text{Se}^0 + 2\text{Cu}^{2+} + 4\text{e}^- \leftrightarrow \text{Cu}_2\text{Se}$ $2\text{CuSe} + 2\text{e}^- \leftrightarrow \text{Cu}_2\text{Se} + \text{Se}^{2-}$ $\text{Se}^{2-} + \text{Cu}^{2+} \rightarrow \text{CuSe}$ $\text{Se}^{2-} + \text{Se}^{4+} \leftrightarrow 2\text{Se}^0$	Stage 2: CuSe, $\text{Cu}_2\text{Se}$ . $\text{Se}^0 + \text{Cu}^{2+} + 2\text{e}^- \leftrightarrow \text{CuSe}$ $\text{Se}^0 + 2\text{Cu}^{2+} + 4\text{e}^- \leftrightarrow \text{Cu}_2\text{Se}$
Stage 3. $\text{In}_2\text{Se}_3$ $3\text{Se}^{2-} + 2\text{In}^{3+} \leftrightarrow \text{In}_2\text{Se}_3$	Stage 3. In and $\text{Cu}_x\text{In}_y + \text{Se}$ $\text{In}^0 + \text{Se}^0 \rightarrow \text{In}_2\text{Se} + \text{InSe} + \text{In}_2\text{Se}_3$ $\text{Cu}_x\text{In}_y + \text{Se}^0 \rightarrow \text{Cu}_{x+z}\text{In}_{y-w} + \text{In}_4\text{Se}_3 + \text{InSe} + \text{Cu}_{2-x}\text{Se} + \text{CuInSe}_2 + \text{Se}$	Stage 3. In and $\text{Cu}_x\text{In}_y + \text{Se}$ $2\text{In}^{3+} + 3\text{Se}^{2-} \rightarrow \text{In}_2\text{Se}_3$ $2\text{In} + 3\text{Se}^{2-} \rightarrow \text{In}_2\text{Se}_3$ $\text{Cu}_x\text{In}_y + \text{Se}^{2-} \rightarrow \text{CuInSe}_2$
Stage 4: In and Cu-In $\text{In}^{3+} + 3\text{e}^- \rightarrow \text{In}^0$ $x\text{In}^{3+} + y\text{Cu}^{2+} \rightarrow \text{Cu}_x\text{In}_y (x>y)$	Stage 4: $\text{CuInSe}_2$ attack $\text{CuInSe}_2 \leftrightarrow \text{Cu}_2\text{Se} + \text{In}_2\text{Se}_3$ .	Stage 4. Crystal growth $\text{Cu}_2\text{Se} + \text{In}_2\text{Se}_3 \rightarrow \text{CuInSe}_2$
Stage 5. $\text{CuInSe}_2$ $\text{Cu}_2\text{Se} + \text{In}_2\text{Se}_3 \leftrightarrow \text{CuInSe}_2$		

The last treatment effectively recrystallizes  $\text{CuInSe}_2$  as noticed in the SEM images and confirmed by XRD.

The formation of  $\text{CuInSe}_2$  during the potential sweep from  $\text{In}_2\text{Se}_3$  and  $\text{Cu}_{2-x}\text{Se}$  has been already reported [4], and also the selenization steps of CuIn alloys to lead  $\text{CuInSe}_2$  [2,3]. The selenization and electrocrystallization reactions proceed by a combination of solid state [9], chemical and electrochemical reactions with different reaction kinetics. The optimization of the proposed treatments has to be done by studying the phase transformations at different potentials and different times.

The effects of ultrasonic irradiation during the electrodeposition and post-deposition treatments include the improved adhesion with respect of no ultrasonic used, the dispersion of the  $\text{H}_2$  bubbles generated during deposition and the continuous supply of reactants to the electrode surface that allow thick (ca. 1 micron, estimated from atomic force microscopy), and uniform films as well as a crystalline deposits and possibly an enhanced diffusion of the elements during electrocrystallization.

Fig. 7 presents the constant wave photoresponse of the films prepared with 1:1:2 Cu:Se:In proportion before and after the selenization and electrocrystallization treatments.

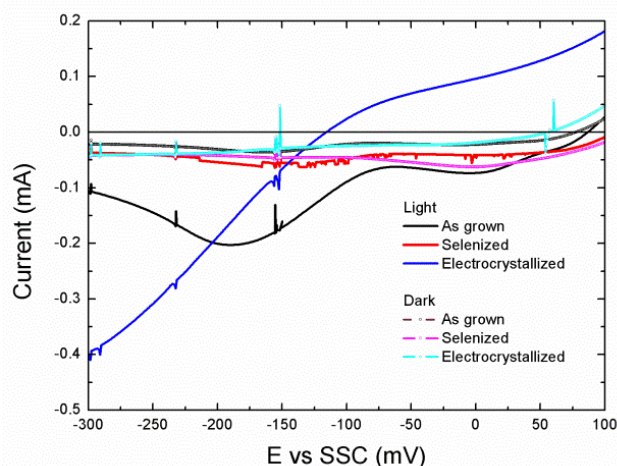


Fig. 7. Photocurrent response of the films prepared in the the 1:1:2 bath, and that of the films with the posdeposition treatments

The as-grown film displays cathodic photoresponse but the peak at about -180 mV indicates further reduction of some of the present phases, possibly Cu-Se.

The formation/exposure of metallic In, Se and Cu-In to the electrolyte damped the photorresponse after selenization. Finally, with the electrocrystallization treatment a response typical of a p-type semiconductor [4] is observed from -100 mV to cathodic potentials, while a positive photocurrent suggests up to +100 mV suggests that observed n-type InSe phases could have a role that deserves to be investigated with more detail in a further work.

#### 4. Conclusions

The results show that compact, adherent  $\text{CuInSe}_2/\text{Cu}$  films with the lowest contents of deleterious phases can be electrodeposited when using a bath with a Cu:Se:In 1:1:2 proportion. Ultrasonic assistance was employed to improve the film homogeneity as well as to keep the deposition rate constant. It was found that an electroless deposited  $\text{Cu}_{2-x}\text{Se}$  film is necessary to ensure CIS adhesion. After the proposed selenization and recrystallization treatments, an as-grown porous deposit evolves to a compact and crystalline film having a reduced amount of deleterious phases and an enhanced photoresponse. This suggests that upon further optimization of the post-deposition treatment conditions, the need of thermal selenization as well as KCN etching could be reduced. However, further work is required to explore the effects of InSe phases on the photovoltaic properties of the materials and to reduce its presence in the films.

#### Acknowledgements

Technical support from F. Rodriguez-Melgarejo@CINVESTAV Qro and SEM Unit at CCiT-UB is acknowledged. Work was financed through CONACYT projects 151679 and 169108 and MICINN-CTQ2012-36090 contract. Potentiostat construction was financed with the SIP-IPN grant 20131877. L.E.A.-R. thanks CONACYT and PIFI for MSc grants and A.P.-P. for a FPU PhD grant.

#### References

- [1] C.J. Hibberd, E. Chassaing, W. Liu, D.B.Mitzi, D. Lincot, D. A.N. Tiwari, Prog. Photovolt: Res. Appl. **18**, 434(2010).

- [2] D. G. Moon, S.J. Ahn, J. H. Yun, A. Cho, J. Gwak, S.K. Ahn, K. Shin, K.Yoon, H.-D. Lee, H. Pak, S. Kwon, *Applied Surface Science* **95**, 2786(2011).
- [3] W. Yanlaia, N. Hongbob, G. Shijuc, **29**, 519(2010).
- [4] J. Kois, O. Volobujeva, S. Bereznev, *Physica Status Solid*, **5**, 3441(2008).
- [5] F. Caballero-Briones, A. Palacios-Adrós, Fausto Sanz, *Electrochimica Acta* **56**, 9556(2011).
- [6] Y. Wang, J. F. Huang, L. Y. Cao, H. Zhu, H. Y. He, J. P. Wu, *Surface Engineering* **27**, 37 (2011).
- [7] V. Sáez, T.J. Mason **4**, 4284(2009).
- [8] K. Ottea, G. Lippoldb, H. Neumannc, A. Schindlera, *Journal of Physics and Chemistry of Solids* **64**, 1641(2003).
- [9] M. Winkler, J. Griesche, I. Konovalov, J. Penndorf, J. Wienke, O. Tober, *Solar Energy* **77**, 705(2004).
- [10] F. Caballero-Briones, A. Palacios-Adrós, J.L. Peña, Fausto Sanz, *Electrochemistry Comm.* **10**,1684(2008).
- [11] A.C. Rastogi, K.S. Balakrishnan, R.K. Sharma, Kiran Jain, *Thin Solid Films* **357**, 179 (1999).
- [12] H. de J. Castillo-Campuzano, L.E. Arvizu-Rodríguez, O. Calzadilla, S. Larramendi, F.J. Espinosa-Faller, F. Chalé-Lara and F. Caballero-Briones, presented at the XIII Simposio y XI Congreso de la Sociedad Cubana de Física, March 16-21, 2014, La Habana, Cuba.
- [13] V. Izquierdo-Roca, X. Fontane, E. Saucedo, J. S. Jaime-Ferrer, J. Alvarez-Garcia, A. Perez-Rodriguez, V. Bermudez, J. R. Morante, *New J. Chem.* **35**, 453(2011).
- [14] C.-M. Xu, X.-L. Xu, J. Xu, X.-J. Yang, J. Zuo, N. Kong, W.-H. Huang, H.-T. Liu, *Semicond. Sci. Technol.* **19**, 1201(2004).
- [15] J. Djordjevic, E. Rudigier, R. Scheer, *J. Crystal Growth* **94**, 218 (2006).